Confinement and Manipulation of Actin Filaments by Electric Fields

Mark E. Arsenault,* Hui Zhao,* Prashant K. Purohit,* Yale E. Goldman,[#] and Haim H. Bau*

*Department of Mechanical Engineering and Applied Mechanics, University of Pennsylvania, Philadelphia, Pennsylvania; and [#]Pennsylvania Muscle Institute, University of Pennsylvania, Philadelphia, Pennsylvania

ABSTRACT   When an AC electric field was applied across a small gap between two metal electrodes elevated above a surface, rhodamine-phalloidin-labeled actin filaments were attracted to the gap and became suspended between the two electrodes. The variance $<s^2(x)>$ of each filament's horizontal, lateral displacement was measured as a function of electric field intensity and position along the filament. $<s^2(x)>$ markedly decreased as the electric field intensity increased. Hypothesizing that the electric field induces tension in the filament, we estimated the tension using a linear, Brownian dynamic model. Our experimental method provides a novel means for trapping and manipulating biological filaments and for probing the surface conductance and mechanical properties of single polymers.

Actin filaments are polymers whose ATP-driven assembly in the cell cytoplasm propels cell shape changes, locomotion, and division. They are also the cytoskeletal tracks for the myosin family of molecular motors, including those for muscle contraction. Given actin filaments' ubiquity, it is not surprising that much work has focused on studying their mechanical (1-3) and electrical (4) properties and the motility of myosin motors along them.
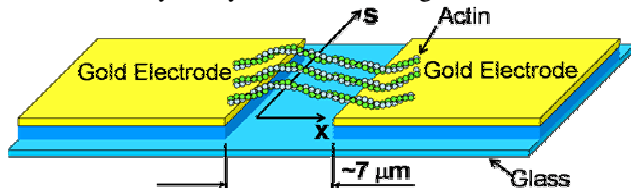

FIGURE 1: A schematic depiction of the experimental apparatus

In order to study the filaments' behavior and interactions with myosin motors, we positioned the filaments at predetermined locations with the aid of electric fields (5, 6). During these experiments, we observed that the amplitudes of the filaments' lateral fluctuations depended strongly on the electric field intensity. This phenomenon appeared sufficiently intriguing to warrant further study.

Our experimental apparatus consisted of a 75 µm-high flow cell sandwiched between two glass slides. Using standard microfabrication techniques, a pair of gold electrodes (10 nm-thick NiCr adhesion layer and 100 nm-thick gold surface layer), with a small gap of ~7 µm between them, was patterned on one of the slides, and a 1 µm-deep trench was etched between the two electrodes to provide free space under the suspended filaments (Fig. 1). The flow cell was filled with a solution of 50 nM rhodamine-phalloidin-stabilized actin, suspended in 37 mM KCl, 2 mM $MgCl_2$, 1 mM EGTA, 20 mM Hepes, and 1 mM DTT (electrical conductivity 0.56 S/m), and was

placed on the stage of an inverted microscope.

When an AC (2 MHz) potential difference was applied across the electrodes, the electric field caused the actin to align parallel to the field lines, migrate towards the maximum electric field intensity, and bridge the gap across the electrodes. This observation is consistent with Asokan et al. (6). Note, however, that Asokan et al. did not suspend the filament above a trench. Fig. 2 is an image of a single filament spanning the gap between the two electrodes.

In contrast to our results, Kobayasi et al. (4) reported optical birefringence measurements suggesting that in a DC field, actin filaments align transverse to the electric field. They speculated that the filaments have a strong, intrinsic dipole moment (of unknown origin) transverse to their long axis. This effect is unlikely to manifest itself in AC fields.

In the absence of the electric field, the filaments settled randomly with just a few filaments anchoring firmly to the gold electrodes. The contour lengths (L) of the filaments' segments confined between the electrodes' edges were typically much larger than the gap's width (G). When the electric field was present, a greater number of filaments bridged the gap between the electrodes, and $L \cong G$.

Once a filament was observed to bridge the gap across the electrodes, an electron multiplying CCD camera (Photometrics Cascade II) took images at 10 Hz. A custom-written Matlab[TM] program was used to obtain the filament's
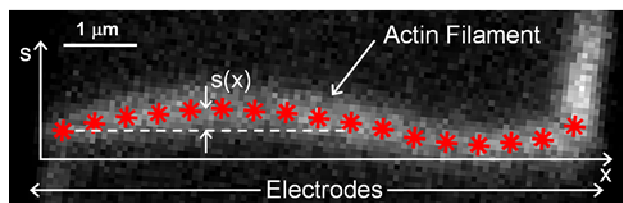

FIGURE 2: Contrast-enhanced image of an actin filament trapped across the gap between two electrodes. The image also depicts the discretized position data (*).
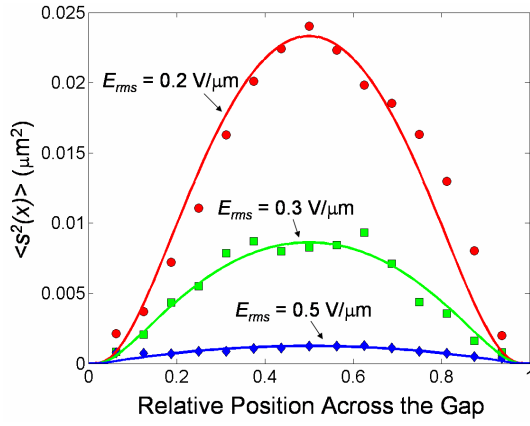
FIGURE 3: The variance of the filament's transverse displacement is plotted vs. relative location across the gap at E_{rms} = 0.2, 0.3 and 0.5 V/μm. The symbols and lines correspond, respectively, to experimental data and theoretical predictions of a tension-optimized, Brownian dynamics-based model for a clamped rod with flexural rigidity $\kappa = 7.3 \cdot 10^{-26}$ Nm^2.

FIGURE 4: The average, standard deviation of the displacement (± 1 s.e.m.) and the filament's estimated tension obtained from Eq. 2 (+ 1 s.e.m., red) and from the clamped model (- 1 s.e.m., blue) (inset) as functions of the square of the electric field intensity. The solid line is the best fit to the clamped model estimates.

displacement $s(x)$ (Fig. 2) as a function of the distance x from one of the anchoring points. The data was then used to compute the variance of the displacement $<s^2(x)>$ as a function of x/G.

A sample of our experimental data obtained with different filaments having similar L/G (<1.01) ratios is given in Fig. 3 at various field intensities. The magnitude of E_{rms} is calculated as the root-mean-square potential difference V_{rms} across the electrodes divided by the gap's width G. As the electric field intensity increases, the variance decreases.

Fig. 4 depicts the normalized standard deviation averaged over the gap's width,

$$\hat{s} = \frac{1}{G}\int_0^G \sqrt{\langle s^2(x)\rangle}dx, \qquad (1)$$

as a function of the electric field intensity squared, E_{rms}^2. The amplitude of the thermal fluctuations decreases markedly as the electric field intensity increases.

This "straightening" effect may result from electric field induced tension that causes transverse torque opposing the filament's bending. To estimate the magnitude of this tension, we modified linear, Brownian dynamics theories of vibrating beams (7) to accommodate beams with uniform effective tension. Using the equi-partition principle, we calculated the asymptotic (long time) value of the variance

$$\left\langle s^2(x)\right\rangle = \sum_{n=1}^{\infty}\left(\frac{2k_BTL^3 \sin^2\left(n\pi x/L\right)}{\tau n^2\pi^2L^2 + \kappa n^4\pi^4}\right) \qquad (2)$$

for a simply supported beam (zero displacement and zero moment at the edges) and for a clamped beam (zero displacement and zero slope at the edges).

In Eq. 2, κ is the flexural rigidity, τ is the apparent tension, T is the temperature, and k_B is the Boltzmann constant. Eq. 2 is based on linear theory that assumes $s \ll L$ and $L \cong G$, as observed for filaments that were trapped in the presence of the electric field. The linear theory applies
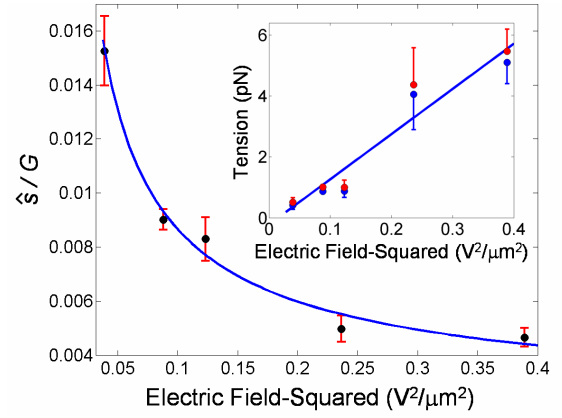
separately to the vertical and horizontal modes of vibrations. The expression for the variance of the clamped beam is lengthy and is given in the on-line Supplementary Information along with the derivation of Eq. 2. The inclinations in the variance data curves at $x = 0$ and $x = G$ suggest that the filaments' boundary conditions were between clamped and simply supported.

Many filaments that settled across the gap in the absence of an electric field significantly deviated from the small-deflection assumption of the linear theory, precluding us from using it to obtain an accurate estimate of κ.

Using a value for the flexural rigidity previously estimated under similar conditions as our experiments, $\kappa = 7.3 \cdot 10^{-26}$ Nm^2 (3), we calculated the apparent tension τ by minimizing the squared difference between the predictions of the beam theories and experimental observations of the variance (Fig. 3). Fig. 4 (inset) depicts the apparent tension estimated from Eq. 2 (red) and the *clamped* model (blue) as functions of E_{rms}^2 for 58 filaments. The estimated tension ranged from 0.5 to 5 pN, was insensitive to the choice of κ, and varied nearly linearly with E_{rms}^2, consistent with forces caused by polarization of the filament and its adjacent electric double layer (EDL).

By what mechanism is the apparent tension generated? One possible contributor to the apparent tension is the polarization of the filament, which induces an effective dipole moment (8). The resulting apparent tension

$$\tau = \chi\frac{2\pi a^2}{3}\varepsilon_m \, \mathrm{Re}\left(\frac{\varepsilon_f^* - \varepsilon_m^*}{\varepsilon_m^*}\right)E_{rms}^2, \qquad (3)$$

where subscripts m and f denote, respectively, the medium and the filament; $a \sim 4$ nm is the filament's radius; $\varepsilon^* = \varepsilon - j\cdot\sigma/\omega$ is the complex dielectric permittivity; ε is the dielectric permittivity; σ is the conductivity, and χ is a constant to adjust for the non-uniformity of the electric field along the filament's length. Through numerical simulations, we estimate $\chi \sim 3$. When $\varepsilon_m = 78\cdot\varepsilon_0$, $\varepsilon_f = 36\cdot\varepsilon_0$

(at the frequency of our experiments, the magnitude of ε_f has an insignificant effect), and $\sigma_m = 0.56$ S/m, we estimate $\tau \cong 1$ pN at $E_{rms} = 0.3$ V/μm. According to Eq. 3, the corresponding $\sigma_f \cong 85$ S/m. In the case of a thin EDL (9), σ_f can be decomposed into three components: (i) the intrinsic conductivity of the filament; (ii) the diffuse layer's conductivity estimated as 0.95 S/m (surface charge of $6.4 \cdot 10^{-19}$ C/nm = 4 e⁻/nm, pH = 7.2, and potassium counterions) (6); and (iii) the stagnant layer's conductivity (for which data is not available). The stagnant layer's conductivity is typically assumed to have a similar magnitude to that of the diffuse layer. Thus, to obtain the estimated tension with Eq. 3, σ_f would need to be nearly two orders of magnitude larger than the estimated contribution of the diffuse layer to the (surface) conductivity of actin filaments.

The EDL in our experiment is quite thick relative to the filament's radius, $\lambda_D/a \sim 0.4$, where λ_D is the Debye screening length. To account for a thick EDL, we calculated the shear stress induced by the flow of ions in the EDL enveloping the filament. The alternating electric field causes the ions in the EDL to migrate from the filament's center towards its ends. The resulting hydrodynamic flow imposes a shear stress along the filament's surface, manifesting itself as apparent tension. This phenomenon also leads to electric current flow along the filament's surface. This current is occasionally approximated as the diffuse layer's contribution to the surface conductivity (9). We computed the ion transport around the filament when the filament's linear charge density is $6.4 \cdot 10^{-19}$ C/nm, the stagnant layer's conductivity is negligible, and $E_{rms} = 0.3$ V/μm, to find that the corresponding viscous forces contribute about 0.01 pN or two orders of magnitude less than the estimated tension. In order to obtain the apparent tension estimated from the experiments, a charge density of $\sim 190 \cdot 10^{-19}$ C/nm would be needed, which is about two orders of magnitude larger than the value calculated from the protein net charge (10).

Of course, there are other induced charges, such as in the EDL along the electrodes (AC electroosmosis, (11)) and in the bulk of the solution (resulting from temperature gradients caused by the microscope's illumination (12)), that will migrate in the electric field and induce fluid motion. At the electric field frequency and solution conductivity of our experiments, AC electroosmosis is negligible. By seeding the fluid with small particles, we visualized the electrothermal convection and found it to be directed upwards in the gap between the electrodes, which would induce slack forces rather than tension.

In summary, we report for the first time on the effect of electric fields on the thermal fluctuations of actin filaments. As the electric field's intensity increases, the amplitude of the filament's lateral fluctuations decreases, and the apparent tension increases. These features are consistent with the electric field affecting the filament's behavior through the polarization of the filament and its surrounding electric double layer. The magnitude of the reduction of the filament's vibrations by the electric field is not quantitatively explained using established values for actin filament properties. According to our analysis, either the intrinsic or the surface conductivity of the filament would need to be several orders of magnitude larger than expected. However there might be other, yet unknown, unaccounted effects that may explain our observations. The simplicity of trapping, observing, and manipulating filaments by electric fields may make this approach useful for further study of the surface properties of polyelectrolytes, for directed assembly of biopolymers, and for motility-based biophysical experiments. Finally, the technique described here provides a novel means to estimate the surface conductivity of single molecules.

SUPPLEMENTARY MATERIAL

Videos of filament fluctuations and detailed derivations can be found by visiting BJ Online at http://www.biophysj.org.

ACKNOWLEDGMENTS

REFERENCES

1. Riveline, D., C., H. Wiggins, R. E. Goldstein, and A. Ott. 1997. Elastohydrodynamic study of actin filaments using fluorescence microscopy. *Phys. Rev. E*. 56:1300–1333.

2. Tsuda, Y., H. Yasutake, A. Ishijima, and T. Yanagida. 1996. Torsional rigidity of single actin filaments and actin-actin bond breaking force under torsion measured directly by in vitro micromanipulation. *Proc. Natl. Acad. Sci. USA*. 93:12937–12942.

3. Gittes, F., B. Mickey, J. Nettleton, and J. Howard. 1993. Flexural rigidity of microtubules and actin filaments measured from thermal fluctuations in shape. *J. Cell Biol*. 120:923–934.

4. Kobayasi S., H. Asai, and F. Oosawa. 1964. Electric Birefringence of Actin. *Biochim. et Biophys. Acta*. 88:528-540.

5. Riegelman, M., H. Liu, and H. H. Bau. 2006. Controlled nanoassembly and construction of nanofluidic devices. *J. Fluids Eng.*. 128:6-13.

6. Asokan, S. B., L. Jawerth, R. L. Carroll, R. E. Cheney, S. Washburn, and R. Superfine. 2003. Two-Dimensional Manipulation and Orientation of Actin-Myosin Systems with Dielectrophoresis. *Nano Letters*. 3:431-437.

7. Van Lear, G. A. and G. E. Uhlenbeck. 1931. The Brownian Motion of Strings and Elastic Rods. *Phys. Rev*. 38:1583-1598.

8. Jones, T., B. 1995. *Electromechanics of Particles*. Cambridge University Press, New York, NY.

9. O'Konski, C. T. 1960. Electric properties of macromolecules. V. theory of ionic polarization in polyelectrolytes. *J. Phys. Chem*. 64:605–619.

10. Tang, J., X. and P. A. Janmey. 1996. The Polyelectrolyte Nature of F-actin and the Mechanism of Actin Bundle Formation. *J. Biol. Chem*. 271:8556-8563.

11. Squires, T. M. and M. Bazant. 2004. Induced-charge electro-osmosis. *J. Fluid Mechanics*. 509:217–252.

12. Green, N. G., A. Ramos, A. Gonzalez, A. Castellanos, and H. Morgan. 2000. Electric field induced fluid flow on microelectrodes: the effect of illumination. *J. Phys. D: Appl. Phys*. 33:L13–L17.